Electronic Supplementary Information

Fast Quantitative Optical Detection of Heat Dissipation by Surface Plasmon Polaritons

Thomas B Möller†[a], Andreas Ganser†[+a], Martina Kratt[a], Simon Dickreuter[§a], Reimar Waitz[$a], E. Scheer[*a], Johannes Boneberg[a] and Paul Leiderer[a]

[a] *Department of Physics, University of Konstanz, 78457 Konstanz, Germany.*
† Both authors contributed equally to the work.
+ Now at: Dep. Mech. Engin., Technical University Munich, 85748 Garching
§ Now at: Inst. Appl. Phys., Eberhard Karls Universität Tübingen, 72076 Tübingen
§ Now at: Rational AG, 86899 Landsberg am Lech
** Corresponding author: elke.scheer@uni-konstanz.de*

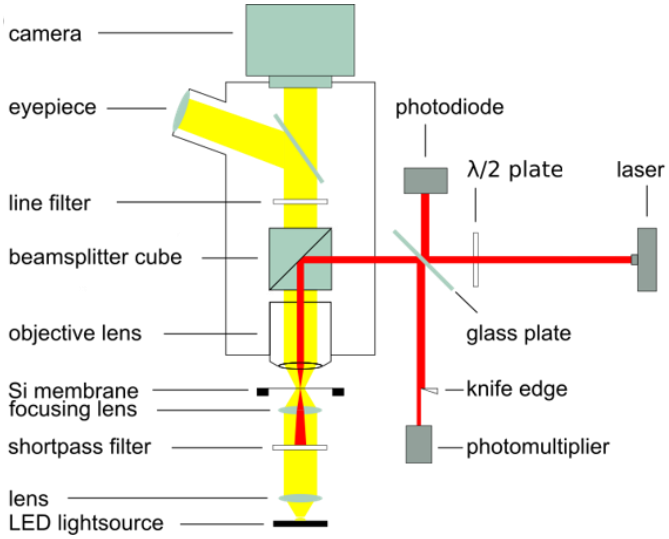

Fig. S1 Optical set-up for the investigation of surface plasmon polaritons. The Si membrane with gold stripe and grating is imaged with an optical resolution of about 0.4 µm onto the chip of a digital camera. The membrane is illuminated from below with a "white light" LED, and with a line filter in the microscope the suitable wavelength for the temperature measurement is selected (488 nm in this case). The beam of a diode laser ($\lambda = 785$ nm), incident on the sample from above, generates SPPs in the gold stripe when focused on the grating. A shortpass filter below the sample prevents laser light which is transmitted through the sample from affecting the LED output. The laser power is monitored using a glass plate beam splitter and a photodiode, and the same beam splitter, together with a photomultiplier and a knife edge, is used to measure part of the laser light reflected from the sample. This allows one to check for membrane oscillations, which are initiated by the pulsed illumination at high laser power. Such membrane oscillations can lead to artefacts in the time-resolved temperature measurements, because they also give rise to slight modulations of the transmitted LED light due to membrane tilt. Some of the "noise" in the data of Fig. 8b is caused actually by such oscillations.

For time-resolved measurements, both the (pump) laser diode and the (probe) LED are operated in a pulsed mode with a variable delay Δt between pump and probe. In this way, a map of the temperature distribution in the membrane can be obtained for every value of Δt. In order to improve the signal-to-noise ratio, these maps are averaged over typically several hundred pulses.

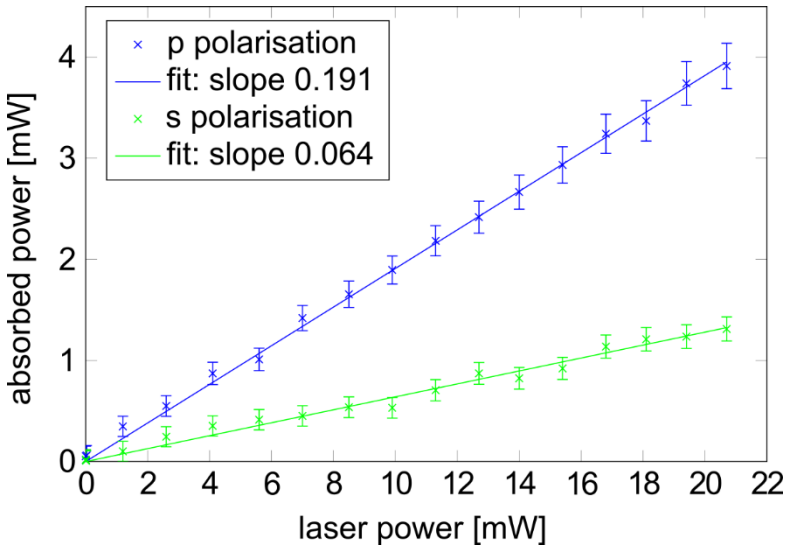

Fig. S2 Comparison of the power dissipated in the grating and the surrounding gold stripe as a function of the incident laser power for the situation depicted in Fig. 2. One notices a linear dependence between the incident optical and the dissipated thermal powers, which is not surprising because nonlinear effects should not be relevant in this intensity range. From the slopes of the two straight lines it follows that the fraction of the incident radiation which is absorbed and eventually transferred into heat is here 6.4% and 19.1% for s and p polarisation, respectively. This demonstrates again the much more efficient coupling to incident radiation when the ridges of the grating are perpendicular to the electric field of the incident light.

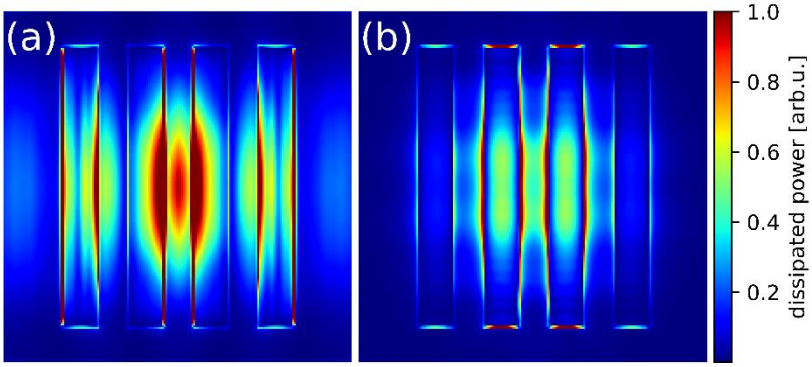

Fig. S3 Influence of the monitor area in the FDTD simulation. Shown is the normalised dissipated power density $P(x,y)$, obtained from a simulation for the gratings used in the experiment. The simulation conditions are the same as for Fig. 4 in the main text, except for the monitor area, which here is confined to the box displayed in the figure, 4x4 μm^2 [38]. Similar to Fig. 4, the color code of the dissipated power density was capped to increase the contrast, but for these images a five times higher threshold than in Fig. 4 was chosen, in order to optimize the visibility of the features inside the gratings. The polarisation of the incident light in (a) is perpendicular to the grating grooves and in (b) parallel to the grooves. The absorptivity determined from this simulation is 12.3% for (a) and 3.2% for (b).

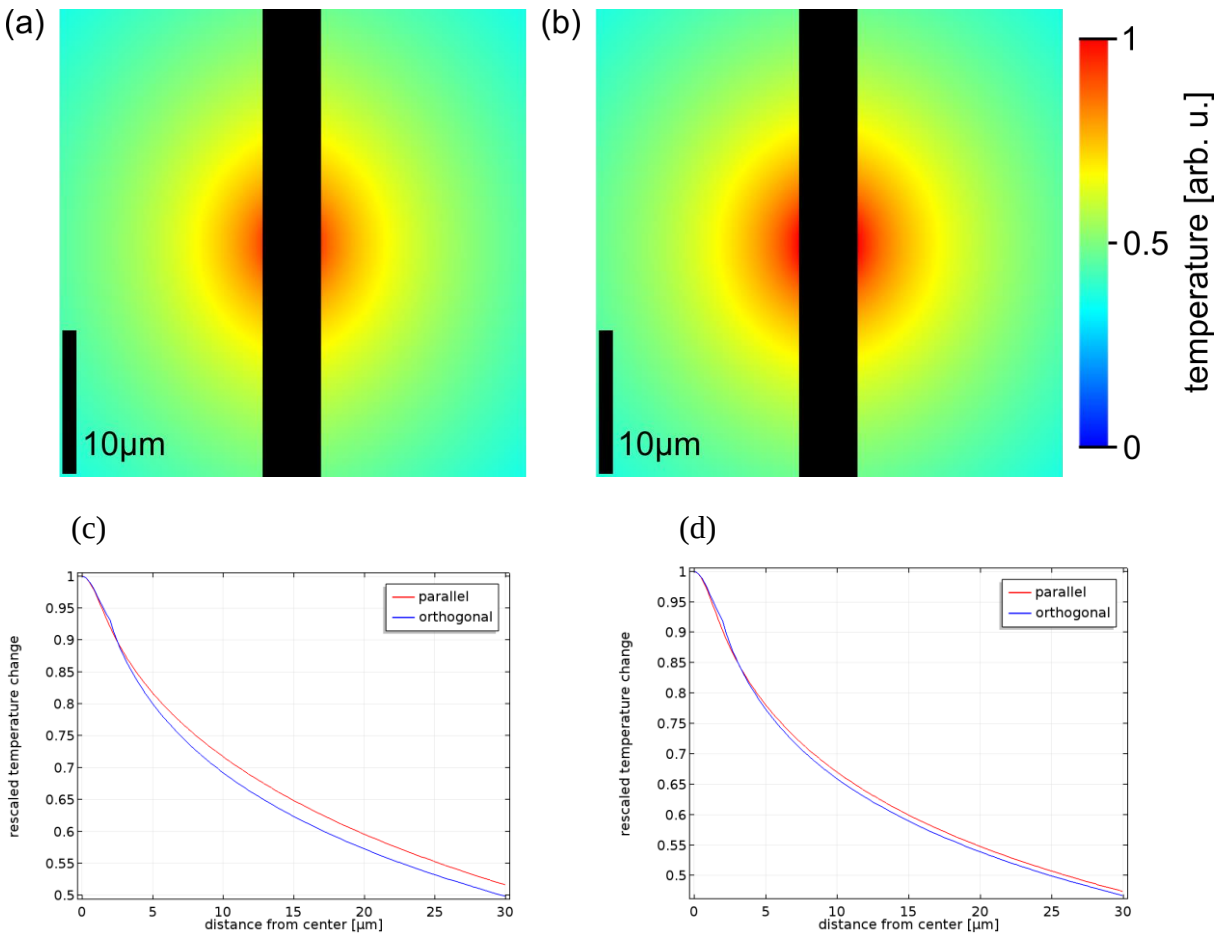

Fig. S4 FE simulations for *steady state* heating. (a) and (b) represent the same data as in Fig. 2 for p- and s-polarisation, respectively, but here in both cases normalized to 1. This allows a better visual comparison of the influence of polarisation on the anisotropy of the temperature map. (c) and (d) are temperature profiles taken parallel and orthogonal to the gold stripe, respectively. At a distance of 20 µm from the center the difference between the temperatures is 3.8% for p- and 1.8% for s-polarisation.

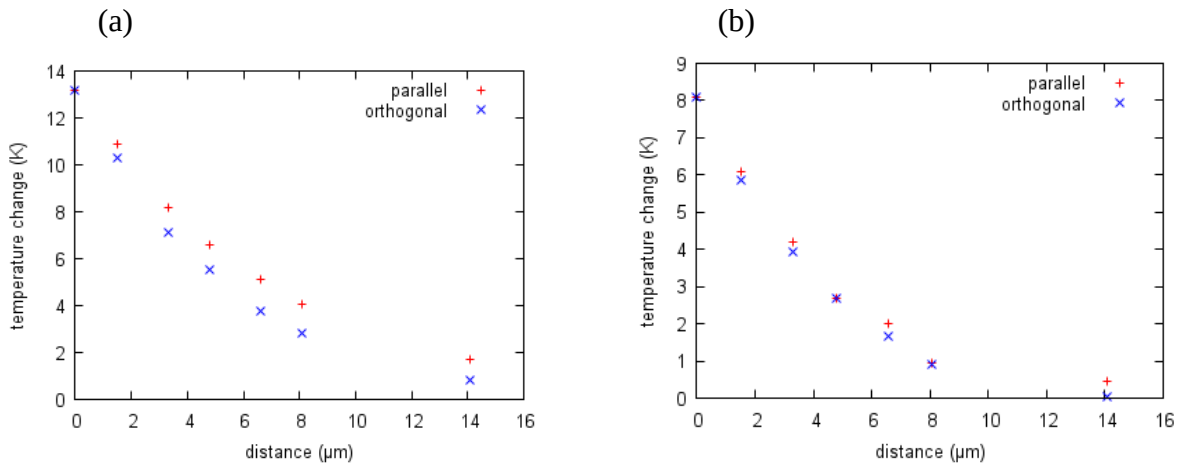

Fig. S5 Experimental temperature profiles for a *pulsed* measurement as in Figs. 6 and 7, taken at a time t = 1 µs after the beginning of the laser pulse. Graph (a) was recorded for illumination with p-polarised laser light, graph (b) for s-polarised light. The data refer to paths parallel (blue) and orthogonal (red) to the gold stripe, along lines through the ROIs indicated in Fig. 8.

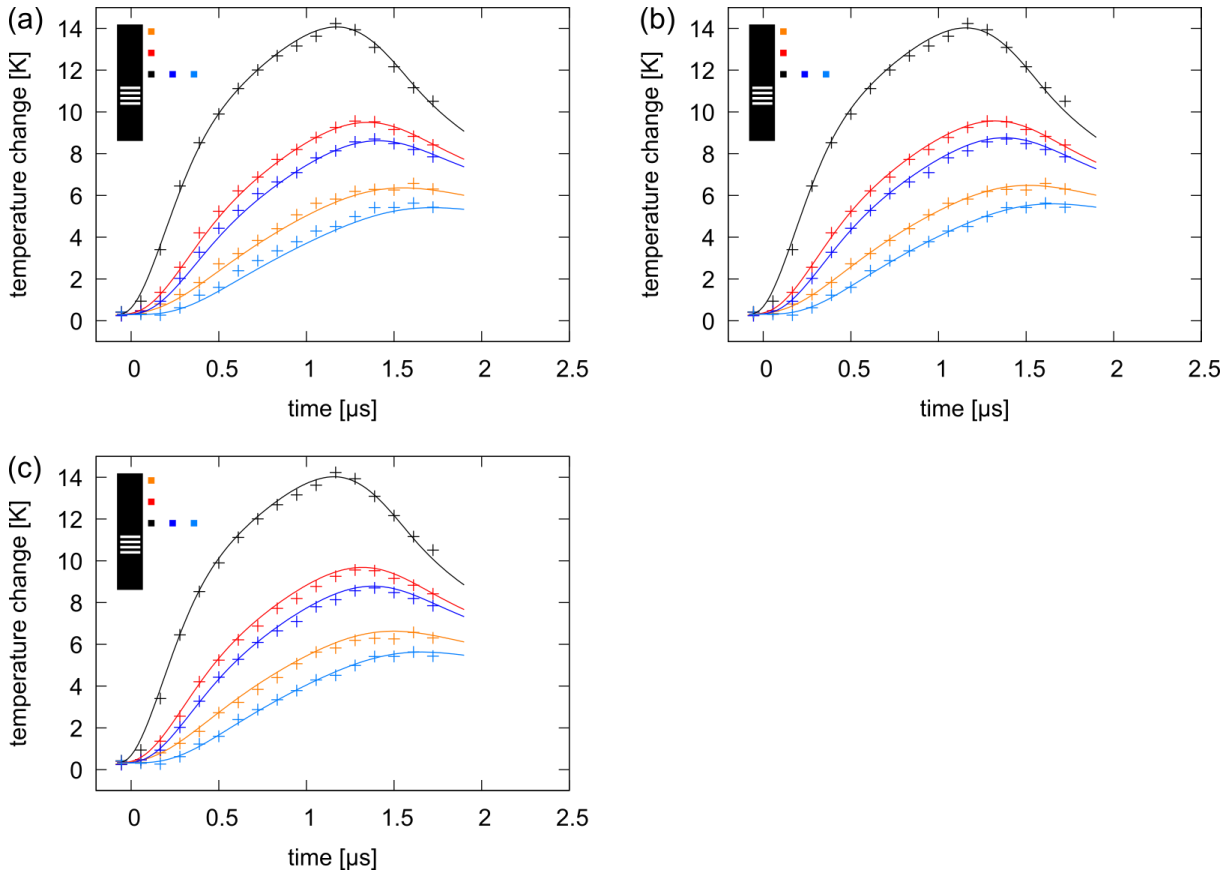

Fig. S6 Determination of the effective thermal conductivity κ of the Si membrane: Comparison of simulations for different values of κ with the experimental data of Fig. 8a. (a) $\kappa/\kappa_{bulk} = 0.40$; (b) $\kappa/\kappa_{bulk} = 0.45$; (c) $\kappa/\kappa_{bulk} = 0.50$. The second parameter in the simulations, the fraction of SPPs, is fixed to 25% in all 3 graphs. The best fit, derived from minimum mean square deviations, is obtained for $\kappa/\kappa_{bulk} = 0.45$. In order to check for a possible mutual dependence of the best fit parameters for $\kappa eff /\kappa_{bulk}$ and the SPP fraction, we have considered also other SPP values, and find that the optimum result for for κ/κ_{bulk} depends only weakly on the choice of the SPP fraction.

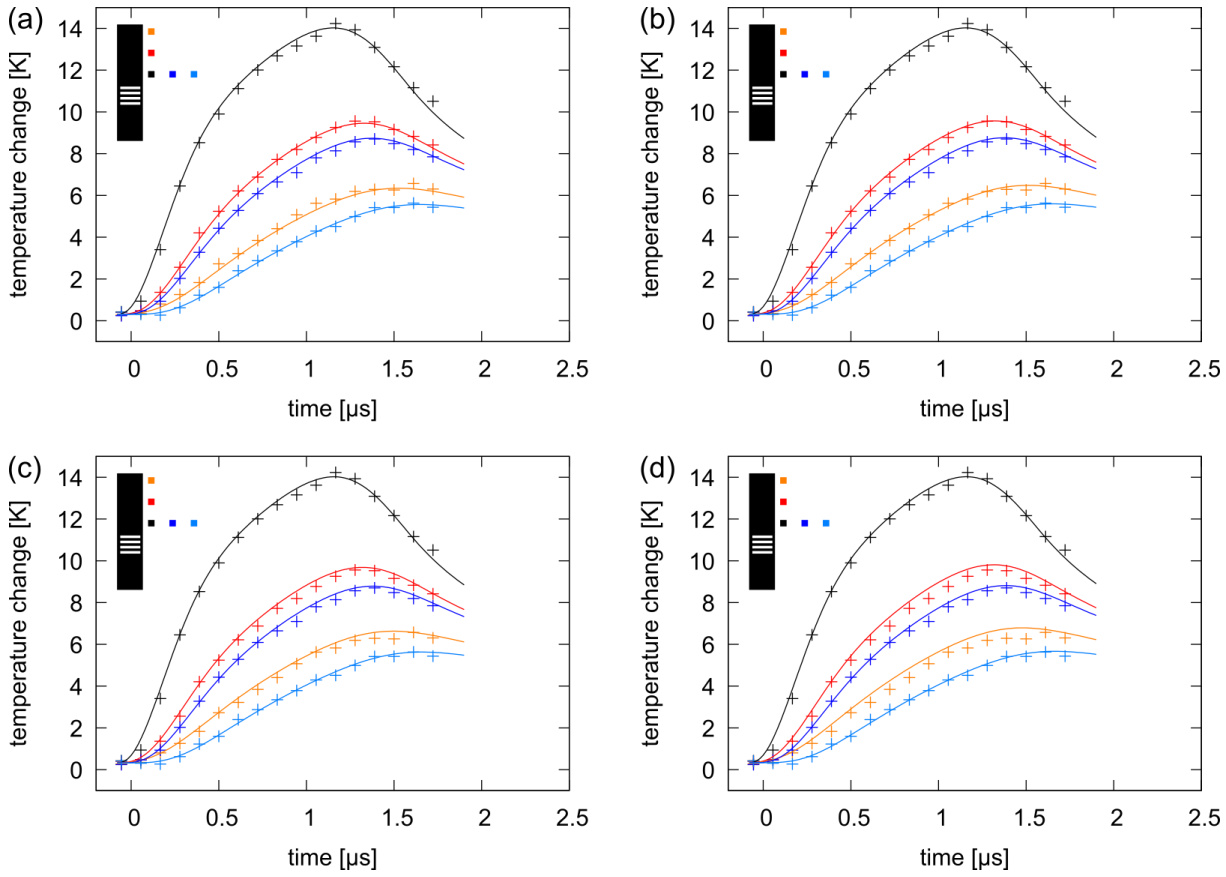

Fig. S7 Comparison of the experimental data of Fig. 8a with simulations for different fractions of SPPs: (a) 20%; (b) 25%; (c) 30%; (d) 35%. The reduced thermal conductivity of the Si membrane is fixed to $\kappa/\kappa_{bulk} = 0.45$ in these simulations. The best fit, derived from minimum mean square deviations, is obtained for an SPP fraction of 25%.

Parameters of the FE simulation

In the FE simulations, the sample is described as follows: The silicon membrane is modelled as a 500x500x0.34 µm box. On top of the membrane box is another 500x4x0.1 µm box to represent the gold stripe. The material parameters for silicon are the heat capacity at constant pressure of 710 J/(kg·K), a density of 2329 kg/m^3 and a thermal conductivity which is one of the free parameters of the simulation. The material parameters for gold are the heat capacity at constant pressure of 129.1 J/(kg·K), a density of 19300 kg/m^3 and a thermal conductivity of 173 W/(m·K). To calculate the temperature distribution, a completely thermally isolated sample is assumed. The heating is done with two heat sources on the top surface of the gold. The first one represents the heat generated by the laser. Its spatial distribution is therefore a Gaussian with a full width at half maximum of 2 µm. The second heat source is the representation of the plasmonic heat contribution. It has the same spatial distribution as the laser source in the direction orthogonal to the stripe, but along the stripe two exponential decays are implemented. The simulation gives a complete temperature distribution in the whole simulated geometry. To compare these results with the experiments, the temperature of the top of the silicon membrane is extracted at the same positions as in the experiment.